

An observational study of the factors that influence interception loss in boreal and temperate forests

T. Toba^{1,a} and T. Ohta^{1, 2, 3, b}

¹ Graduate School of Bioagricultural Sciences, Nagoya University, Nagoya 464-8601, Japan

² Frontier Observational Research Systems for Global Change, Yokohama 236-0001, Japan

³ Japan Science and Technology Agency/CREST, Kawaguchi 332-0012, Japan

Author for correspondence

^a Fax: +81-52-789-5038

E-mail: i011007d@mbox.nagoya-u.ac.jp (T. Toba)

takeshi@agr.nagoya-u.ac.jp (T. Ohta)

^b Fax: +81-52-789-4059

Abstract

This study used same methods to observe interception loss in two boreal forest sites in Siberia and five temperate forest sites in Japan; interception characteristics of the two climate regions were compared. The Siberian sites had high interception ratios of 0.2–0.3. In contrast, the Japanese sites had low interception ratios of ca. 0.15 in coniferous forests and 0.2 in broadleaf forests. Although interception loss generally increases with the plant area index (PAI), our data showed the opposite trend. This suggests that meteorological variables had a greater effect on interception loss than did differences in canopy structure. Rainfall characteristics appeared to be the main meteorological factor affecting interception loss. When mean rainfall intensity exceeded 1 mm hr^{-1} , the interception ratio remained near the upper limit of 0.2 regardless of other rainfall conditions. In contrast, windy and drier atmospheric conditions strongly affected the interception rate when the rainfall intensity dropped below 1 mm hr^{-1} .

Japan and Siberia showed significant energy-balance differences related to evaporation from wet canopies. At the Siberian sites, the net all-wave radiation was always larger than the latent heat flux used for interception loss, while Japanese sites often showed the opposite pattern. When the latent heat flux exceeded the net all-wave radiation, the air temperature above the canopy during rainfall events was higher at upper levels than at lower levels, even in the daytime. These results indicate that the sensible heat flux was directed downward and suggest that both net all-wave radiation and sensible heat flux contribute to evaporation from wet canopies during and shortly after rainfall events in Japan.

Key words: interception loss; rainfall characteristics; forest structure; boreal and temperate forest; energy budget

1. Introduction

Interception loss plays an important role in hydrological processes, especially in forests. To evaluate forest evapotranspiration, it is necessary to clarify the important characteristics of interception loss.

Observational studies of interception loss fall into several categories. Many researchers have focused on rainfall conditions. For example, in dry atmospheric conditions, interception rates are primarily controlled by rainfall intensity (Llorens *et al.*, 1997). Tsukamoto *et al.* (1988) also found that the interception rate increased proportionately with rainfall intensity of less than 7.0 mm hr^{-1} . However, the relationships among rainfall intensity, duration of rainfall events, and other weather elements are not clear. Researchers have also examined the relationship between wind speed and interception loss. For example, high wind speeds could theoretically orient leaves parallel to the wind and reduce the probability of interception. However, in tropical rainforests with dense canopies, the probability of a raindrop passing through the canopy without contacting a vegetative surface is relatively low even under strong wind conditions (Herwitz and Slye, 1995). Little research has focused on differences between broadleaf and coniferous forests, differences in crown density, and differences between sparse and dense forests. Lastly, researchers have examined methods with which to measure and analyze rainfall, throughfall, and stemflow. The position and height of rainfall and throughfall collectors and gauges affect the observed values (Crockford and Richardson, 2000; Kuraji and Tanaka, 2003), and differences in setup times for recording a single event can also influence the observed interception loss (Llorens *et al.*, 1997). Previous research has shown that unifying the observation and analysis methods is important in comparing interception characteristics among several sites.

Observational data have improved interception models. Numerical models have also been developed to calculate interception loss. These include analytical (Gash, 1979; Gash *et al.*, 1995; Carlyle-Moses and Price, 1999), tank (Rutter *et al.*, 1971; Hashino *et al.*, 2002), and physically based interception (Liu, 1997) models.

Numerous observation- and model-based studies have examined low-latitude tropical forests (Herwitz and Slye, 1995; Asdak *et al.*, 1998; Hutjest *et al.*, 1990; Jetten, 1996) and mid-latitude temperate forests (Link *et al.*, in press; Llorens and Gallart, 2000; Gómez *et al.*, 2001). However, observations of interception losses in high-latitude boreal forests are lacking. For comparative examinations of low-, mid-, and high-latitudes, a universal model is needed to estimate the amount of interception loss over a wide area.

To improve modeling results, researchers have examined diurnal variation or time series of interception loss in arid and semi-arid areas using interception models (Asdak *et al.*, 1998; Hutjest *et al.*, 1990). Herwitz and Slye (1995) found that the amount of interception loss was strongly affected by the position of the adjusting trees. Further, Link *et al.* (in press) simulated a time series of interception loss using a physical model and noted the importance of canopy storage capacity.

The characteristics of water cycles at low-, mid-, and high-latitudes differ (Kelliher *et al.*, 1998; Ohta *et al.*, 2001). Many researchers have compared water exchange above dry canopies in different latitude belts, but few have observed water exchange above a wet canopy at high latitudes, and none have compared water exchange above wet canopies among latitude belts. While many interception-loss studies have focused on tropical and temperate forests, few have examined the interception-loss characteristics of high-latitude boreal forests. Moreover, no observations of interception loss have been made in the Siberian taiga. The characteristics of interception loss under the peculiar weather conditions of the subarctic zone, i.e., dry with little rain, are needed to compare water cycle characteristics among different climate zones. Further, few studies have examined interception loss under different climatic conditions using the same observation methods. Therefore, as Crockford and Richardson (2000) pointed out, it is

important to use the same observation system when discussing the spatial distribution of interception loss characteristics.

This study examined the characteristics of interception loss in eastern Siberia and Japan. Here we clarify the relationship between interception loss and meteorological conditions or forest structure for Siberian boreal forests and Japanese temperate forests, examine the difference in interception characteristics between Siberia and Japan, and compare the energy balance of interception loss in each region.

2. Site descriptions

Observations were made in Siberia and Japan. Two sites were established in one area in Siberia, and five sites were established in two areas in Japan.

2.1. Siberia

The two Siberian observation sites were located near the city of Yakutsk, along the middle reaches of the Lena River. Site P4 contained red pine (*Pinus sylvestris*), while site L1 was dominated by larch (*Larix cajanderi*), and both sites were situated on the west bank of the Lena River (62°15' N, 129°37' E). Site L1 had a stand density of 840 stems ha⁻¹, a mean stand height of 18 m, and a plant area index (PAI) of 3.71 during the foliated season. Site P4 had a stand density of 1,492 stems ha⁻¹, a mean stand height of 10 m, and a PAI of 2.80. Both sites had sparse understory vegetation, and the canopies consisted of overstory trees only.

2.2. Japan

The Japanese study sites were located in northern and central Japan. In northern Japan, sites P1, P2, and P3 consisted of red pine (*Pinus densiflora*). These sites were situated 25 km west of Morioka (39°40' N, 140°56' E). Site P1 had a stand density of 1,444 stems ha⁻¹, a mean stand height of 11 m, and a PAI of 4.44. Site P2 had a stand density of 1,678 stems ha⁻¹, a mean stand height of 13 m, and a PAI of 4.25 during the foliated season. Site P3 had a stand density of 355 stems ha⁻¹, a mean stand height of 23 m, and a PAI of 3.74. Sites P1 and P3 consisted of pine only, whereas site P2 had an understory that included *Alnus hirsuta*, *Prunus grayana*, and *Styrax japonica*.

The two sites in central Japan were dominated by deciduous broadleaf forests. Site Qa, located 20 km west of Nagoya (35°10' N, 137°11' E), consisted of sawtooth oak (*Quercus acutissima*) and had no understory vegetation. The site had a stand density of 350 stems ha⁻¹, a mean stand height of 14 m, and a PAI of 3.54 during foliation. Oak (*Quercus serrata*) dominated site Qs, which was located near the center of Nagoya (35°9' N, 136°58' E). This site had a stand density of 2,852 stems ha⁻¹, a mean overstory stand height of 18 m, and a PAI of 5.18 during foliation. *Cleyera japonica*, *Ilex pedunculosa*, and *Evodiopanax innovans* were the primary species in the understory. Table 1 summarizes the vegetation parameters, meteorological conditions, and observation periods at all sites.

3. Methods

3.1. Throughfall

U-shaped troughs with 0.2 × 2-m openings and depths of 10 cm were used to collect throughfall at all sites except Qa, where circular trays 0.36 m in diameter were used. The collectors were installed approximately 0.8 m above the forest floor and were inclined 5–13° from the horizontal. The volume of the throughfall collected by the troughs was measured using tipping buckets with a volume of 15.7 ml or stored in collector buckets. The tipping buckets provided automatic measurements of throughfall, and data loggers recorded throughfall at 10-minute intervals. The buckets were used to measure the throughfall amount for each rainfall event, and each trough or tray had a tipping bucket or storage bucket installed.

Sites L1, P1, P3, and P4 had only storage buckets. Sites P2 and Qs had both tipping buckets and storage buckets, while Qa had only tipping buckets. Table 1 shows the number of collectors at each site. The average value of throughfall obtained by each collector, which was divided by the active area of collectors, was used as the spatial mean throughfall.

Tipping-bucket values tend to be underestimated as the input volume increases (Shiraki, 2004). Because of their large catchment area, the actual input volume from troughs and trays can exceed the values recorded in the loggers used for rainfall measurements. Throughfall data measured by the gauges were adjusted using the following equation (Shiraki, 1997):

$$F = 1.4(\sqrt{f + 0.1}) + 15.17, \quad (1)$$

where F is the actual volume needed for one tip (ml), and f represents the observed value obtained by the 15.7-ml tipping bucket per unit of time (ml sec⁻¹).

3.2. Stemflow

The stemflow collectors consisted of rubber hose or polyurethane foam rings that were sealed with silicone rubber to form a watertight junction between the collectors and the tree bark. The collectors encircled the trunk at least 1.5 times.

The same measuring and data-logging methods used to measure throughfall were used to observe stemflow. One tipping bucket or one storage bucket was installed at each sampled tree (Table 1). The average value of stemflow obtained by each collector, which was divided by the crown area of each tree, was used as the spatial mean stemflow. Stemflow data, obtained from tipping buckets with an accuracy of 15.7 ml, were adjusted with the same method used for throughfall expressed in equation (1).

3.3. Gross rainfall

Gross rainfall measurements for sites L1 and P4 were made at open areas located 1 and 1.6 km from the respective sites. As rainfall intensity in Siberia is usually low, the rain gauges at this site had a large catchment area, with a diameter of 0.4 m and measurement resolution of 0.125 mm. The data logger stored data at 1-hour intervals for sites L1 and P4.

Gross rainfall measurements for sites P1, P2, and P3 were made in an open area approximately 200 m from each site, and data for sites Qs and Qa were collected in open sites approximately 100 m from each site. Two rain gauges with 0.5- and 0.2-mm resolution were used at these sites in northern and central Japan. Data loggers stored data at 10-minute intervals. Data from the 0.5-mm tipping-bucket rain gauges were used to calculate the gross rainfall amount for each rainfall event. Hourly hyetographs were made using the temporal distributions observed by the 0.2-mm tipping buckets, based on the amounts obtained from the 0.5-mm tipping-bucket rain gauges.

3.4. Heat pulse speed

The relationship between heat pulse speed and the volume of water uptake is usually required to estimate transpiration rates. Under wet canopy conditions, stomata may close, halting sap flow. The heat pulse method is available to estimate the starting and stopping times of sap flow. We required only the canopy condition (wet or dry) and used the heat pulse method to estimate canopy drying times. Table 1 shows the number of sample trees with heat pulse sensors at each site.

3.5. Meteorological data

Planetary boundary layer (PBL) towers were used to measure meteorological variables above the canopies at P2, P4, L1, and Qs. We measured air temperature, relative humidity, wind speed, and net all-wave radiation above each canopy. Table 2 summarizes the meteorological variables.

Air temperature above the canopy was measured at two or more heights at L1, P2, and P4. To ensure sufficient calibration, an Assmann psychrometer calibrated by the Japan Meteorological Agency was used to adjust air temperature and relative humidity measured automatically at these sites. Time series of air-temperature profiles for the sites were obtained from the data calibrated using the psychrometer.

4. Results

The data obtained in this study from heat pulse measurements showed that canopies took at most 10 hours to dry after rainfall. Therefore, rainfall events separated by more than 10 hours were regarded as independent events in this study.

4.1. Throughfall and stemflow at each site

Table 2 shows the ratio of throughfall and stemflow to gross rainfall at each site. The ratio of throughfall to rainfall (throughfall rate) was small, 0.64 to 0.72, at L1, P4, and Qa, and the other four sites had rates of about 0.80. Moreover, the ratio of stemflow to rainfall (stemflow rate) at the two Siberian sites was extremely low and was about 0.04 at the five sites in Japan.

We considered the relationships between gross rainfall and throughfall and between gross rainfall and stemflow for all seven sites. The relationships at each site could be approximated using linear relations, and the regression lines for gross rainfall and throughfall for every site showed relatively similar slopes. However, the regression lines reflecting the relationship between gross rainfall and stemflow had very low slopes at L1 and P4 in Siberia and a large slope at P1 in Japan. The slope was 0.62×10^{-4} at L1, 0.31×10^{-3} at P4, and 0.16 at P1. Slopes ranged from 0.19×10^{-1} to 0.49×10^{-1} at the other sites.

The x-section of the regression lines for the relationship between gross rainfall and throughfall or stemflow at every site means the average values of rainfall amount required to occur throughfall or stemflow in which interception loss is included. On the other hand, the y-sections of these relationships denote the water capacity of the canopy or trunks. The relations between the y-section of regressions for throughfall and stemflow and the stand density, tree height, and PAI of every plot were examined. PAI was proportional to the y-section for throughfall and stemflow (Fig. 1), but there were no remarkable relationships between the properties of throughfall, stemflow, and other forest structure variables such as stand density, tree height, and DBH. The canopy capacities for both throughfall and stemflow were affected by PAI.

4.2. Interception loss at each site

The interception loss at each site was calculated using the following equation:

$$I = Pr - T - S, \quad (2)$$

where I is the interception loss (mm), Pr is gross rainfall (mm), T is throughfall (mm), and S is stemflow(mm). Table 2 shows the ratio of interception loss to gross rainfall at each site. At L1, P4, and Qa, the ratio of interception loss to gross rainfall (interception rate) was high. At L1 and P4, both the throughfall and stemflow rates were low, while at Qa, only the throughfall rate was low. Rainfall duration was shorter at these three sites than at the other sites (Table 2).

4.3 Relationships between rainfall characteristics and interception rate

The relationships between the interception rate and the gross rainfall characteristics of each rainfall event for all seven sites were considered. The interception rate decreased exponentially with increasing gross rainfall amounts (see Fig. 3 [a]). The interception loss rates were widely dispersed when gross rainfall values were small, but the interception rate

converged at the upper limit of about 0.2 as gross rainfall increased. These results agree with those of Llorens *et al.* (1997) for a conifer forest and Carlyle-Moses (2004) for a broadleaf forest; these researchers found that the interception rate remained constant, at about 0.2, with higher gross rainfall. The upper limit of the interception rate to gross rainfall dropped from 0.6 to 0.2 when the gross rainfall amount reached 40 mm; small amounts of rainfall caused high interception rates. At 40 mm or more gross rainfall, the interception loss rates were low and remained constant, with an upper limit of approximately 0.2, as mentioned above. This result was observed both in Siberia and Japan regardless of differences in forest structure and climate, although only a few rainfall events exceeded 40 mm in Siberia.

The interception rate varied inversely with the duration of rainfall events. Longer rainfall events had smaller interception rates (see Fig. 3 [b]). When rainfall was short and light, interception rates were widely dispersed.

For each event, interception loss decreased exponentially as the mean rainfall intensity increased (Fig. 2). This relationship differs from the conclusions of Tsukamoto *et al.* (1988), who measured hourly interception rates for a single tree and found that the rate was proportional, *i.e.*, it increased with rainfall intensity when the intensity was less than 7.0 mm hr⁻¹. The result shown in Fig. 2 is opposite to that reported by Tsukamoto *et al.* (1988). Tsukamoto *et al.* (1988) focused on hourly values, whereas we worked with the average values for each event. In addition, Tsukamoto *et al.* (1988) examined only weak rainfall intensities, while we included higher hourly intensities during rainfall events.

We found that interception rates decreased exponentially with amount, duration, and intensity of rainfall. Figure 3(a) and (b) shows the relationship between interception rate and rainfall characteristics and the amounts and duration of rainfall; symbols indicate mean rainfall intensity. Rates were widely scattered for gross rainfall of less than 40 mm and for short rainfall events with intensities of 1.0 mm hr⁻¹ or less. Conversely, during heavy rainfall greater than 1 mm hr⁻¹, interception rates remained approximately 0.2 in Siberia and Japan. When the mean rainfall intensity was 1 mm hr⁻¹ or more, interception rates stabilized near the upper limit of 0.2, regardless of rainfall duration or intensity in both areas. In the light of these results, a key question is to determine which factors affect the interception rate during light rainfall of less than 1 mm hr⁻¹ intensity.

4.4. Relationships between meteorological variables and interception rates

We found no significant relationship between the atmospheric saturation deficit and interception rate for all rainfall events observed, although the atmospheric saturation deficit is usually an important factor for evaporation. Figure 4 illustrates the relationship between wind speed and interception rate for each event. These relationships were basically proportional. The wind speed at P2 and Qs in Japan was low, while the wind speed was high at the Siberian sites L1 and P4. Other factors may thus have caused the wide range in the interception rate.

4.5 Relationship between PAI and interception loss

Figure 5 shows the relationship between the PAI and the average interception rate obtained from this and other studies. Based on our study, the interception rate was inversely proportional to PAI. However, except for sites L1 and P4 in Siberia, our results are within the same range as the other studies. This result implies that the effects of forest structure differ in different climatic zones. Climate conditions differ significantly between Siberia and warm and humid regions such as Japan, which may experience higher interception losses.

4.6 Energy balance perspective

In this section, we analyze the characteristics of interception loss in Siberia and Japan from the viewpoint of the energy balance above the canopy.

The sum of the latent heat flux used for interception loss at each event is defined using the following equation:

$$LH = \lambda \cdot Ic , \quad (3)$$

where LH is the sum of the latent heat flux (MJ m^{-2}), λ is the latent heat of water (MJ kg^{-1}), and Ic is the interception loss for each event (kg m^{-2}).

Heat pulse measurement data revealed that on average, canopies dried 5 hours after rainfall ended. Therefore, analysis of the energy balance covers the start of rainfall to 5 hours after rainfall has ended. Figure 6 plots the sum of the net all-wave radiation during and 5 hours after rainfall against the sum of the latent heat flux obtained from equation (3). For most of the rainfall events at the Siberian sites (L1 and P4), the sum of the net all-wave radiation exceeded the sum of the latent heat flux. However, the opposite was true at the Japanese sites P2 and Qs.

The direction of the sensible heat flux helps explain why Japan and Siberia had different interception characteristics from the standpoint of the energy balance. Temperature profiles above the canopies were examined to estimate the direction of sensible heat flux, because ultrasonic anemometer measurements of sensible heat fluxes were not available under rainy conditions. Figure 7 shows examples of hourly hyetographs and the time series of air temperature differences between two levels above the canopy. The air-temperature difference shown in this figure reflects the upper-level temperature minus the lower-level temperature. Lower-level air temperatures exceeded upper-level temperatures during daytime events at L1 and P4 in Siberia. Thus, the sensible heat flux flowed upward during daytime rainfall events. However, the opposite was true during daytime events at P2 in Japan; at this site, the sensible heat flux moved downward during rainfall events, even in the daytime. These results suggest that in Japan, both net all-wave radiation and sensible heat flux contribute to evaporation from the wet canopy. Other researchers have found similar results in tropical forests (e.g., Shuttleworth *et al.* 1984, 1991). Recently, Takanashi *et al.* (2003) measured the downward sensible heat flux during rainfall in western Japan, and the results indicate that a downward sensible heat flux often occurs in temperate forests even during daytime rain. When examining data from an energy budget perspective, significant differences in the interception loss mechanism are apparent for the Siberian and Japanese sites, although the relationships between interception and rainfall characteristics are similar in both areas.

5. Discussion

Figure 5 indicates that the interception rate increases with PAI. However, as mentioned in Section 4.5 above, the results obtained in our study showed the opposite relationship. The rates found in our study are approximately two-fold higher than interception rates obtained from other studies in which PAI values were similar to those at the Siberian sites. This suggests that meteorological conditions had a greater impact than canopy structure on the interception characteristics at these study sites.

5.1 Interception rate characteristics

The interception rate was 0.2 or less at a rainfall intensity of 1 mm hr^{-1} or less, regardless of tree species or area (see Fig. 2). As shown in Fig. 2, high interception-rate change occurred when rainfall intensity was 1 mm hr^{-1} or less. We examined the weather elements that influenced the interception rate when rainfall intensity was weak. Figure 8 shows the relationship between the interception rate and the saturation deficit divided by wind speed when rainfall intensity was 1 mm hr^{-1} or less. This figure illustrates how the interception rate increased under large saturation-deficit conditions in low-intensity events. The results also indicate that the interception rate was basically higher in strong wind conditions (more than 2 m sec^{-1}) than in weak wind conditions. Therefore, when rainfall intensity was 1 mm hr^{-1} or less, the

saturation deficit affected the interception rate, although no remarkable relationship between interception rate and saturation deficit was found, as mentioned in Section 4.4. Saturation deficit also had a greater effect on interception loss under windy conditions. At sites L1, P4, P2, and Qs, where meteorological conditions were observed, average interception rates ranged in the following order from highest to lowest: P4, L1 (Siberian conifer forests), Qs, and P2 (Japanese broadleaf and coniferous forests, respectively). Rates were around 0.2 at sites P2 and Qs, because the average rainfall intensity exceeded 1.0 mm hr^{-1} . In contrast, rates at sites L1 and P4 were higher than 0.2 because high wind speed caused low rainfall interceptions, although there was no difference in the saturation deficit.

5.2 Interception loss characteristics at Siberian and Japanese sites from an energy exchange perspective

This section summarizes the interception loss in Siberia and Japan from an energy balance perspective. As mentioned in Section 4.6, the sum of net all-wave radiation during and for 5 hours after a rainfall event exceeded the latent heat flux used for evaporation from the wet canopies at the Siberian sites, while the opposite often occurred at the Japanese sites. This indicates that the energy needed for evaporation from a wet canopy exceeded the available energy, and sensible heat flux may provide part of the energy needed for evaporation at the Japanese site. Profiles of air temperatures above the canopies support this hypothesis (see Fig. 7). Both the results obtained from this study in northern and central Japanese sites and the research of Takanashi *et al.* (2003) in western Japan agree with research on tropical forests (Shuttleworth *et al.* 1984, 1991). Temperate and tropical forests have nearly closed canopies, and most energy exchanges take place in the canopy. In contrast, boreal forests have fairly sparse canopies. Energy exchange occurs not only in the forest canopy, but also on the forest floor. Other researchers have also pointed out the importance of water and energy exchanges above the forest floor in Siberian forests (Kelliher *et al.*, 1998; Ohta *et al.*, 2001; Hamada *et al.*, 2004). The relationships between the characteristics of rainfall and meteorology and the characteristics of interception loss show similar tendencies in Siberia and Japan, as mentioned in the previous chapter, but the mechanism of interception loss via the energy balance in these two areas is quite different. Although energy exchanges at the forest floor during rainfall events are beyond the scope of this paper, the water and energy exchange system of the forest floor may affect the energy budgets of the entire forest ecosystem in Siberia.

6. Conclusions

This research investigated the variables that affect interception loss, including meteorological factors and forest structure, in two Siberian forests and five Japanese forests. The study presents the following new interpretations.

The Siberian sites had high interception rates of 0.2–0.3. The Japanese sites had lower interception rates of approximately 0.15 in the coniferous forests and 0.2 in the broadleaf forests. The interception loss rates for each rainfall event decreased with the amount of increasing gross rainfall, rainfall duration, and rainfall intensity. When the mean rainfall intensity exceeded 1 mm hr^{-1} or the gross rainfall exceeded 40 mm, the interception rate remained at the upper limit of 0.2 regardless of the other rainfall conditions. In contrast, windy and drier atmospheric conditions strongly affected the interception rate when the rainfall intensity dropped below 1 mm hr^{-1} .

In general, interception loss increases with the PAI; however, our data indicated the opposite tendency. This suggests that the differences in meteorological variables between Siberia and Japan had a greater effect on interception loss than did the differences in canopy

structure.

The Siberian sites had relatively high saturation deficits and wind speeds, both of which contributed to high interception rates. The Japanese broadleaf forest sites had high rainfall intensities of 2.3 mm hr^{-1} . Consequently, these sites had interception rates of approximately 0.2. In the Japanese conifer forest, the interception rate depended on rainfall intensity; at site P2, the rate was about 0.2. The rainfall intensity at P1 and P3 was 1 mm hr^{-1} or more, but the interception rate was small. Since the threshold level was 1 mm hr^{-1} , other weather elements may have also influenced the rate. However, other weather elements were not measured, and thus the exact cause is unknown.

The sum of the net all-wave radiation during and just after rainfall events exceeded the sum of the latent heat flux in Siberia, but the opposite was true in Japan. Air temperature profiles above the canopies support these results; these profiles suggest that sensible heat flux moves upward during daytime rainfall events in Siberia, but downward during daytime rainfall events in Japan. This means that the net all-wave radiation can be partitioned into sensible and latent heat fluxes in Siberia. In Japan, however, both net all-wave radiation and sensible heat flux contribute to evaporation from a wet canopy.

Acknowledgments

Observations in Siberia were carried out as part of the Global Energy and Water Experiment (GEWEX) Asian Monsoon Experiment–Siberia (GAME–Siberia). The authors thank all the GAME–Siberia members for their kind support and assistance. The authors would also like to thank the editor and the anonymous referees for their helpful and constructive comments.

References

- Asdak, C., Jarvis, P. G., van Gardingen, P., Fraser, A., 1998. Rainfall interception loss in unlogged and logged forest areas of Central Kalimantan, Indonesia. *J. Hydrol.* 206, 237–244.
- Cape, J. N., Brown, A. H. F., Robertson, S. M. C., Howson, G., Paterson, I. S., 1991. Interspecies comparisons of throughfall and stemflow at three sites in northern Britain. *Forest Ecology and Management* 46, 165–177.
- Carlyle-Moses, D. E. 2004. Throughfall, stemflow, and canopy interception loss fluxes in a semi-arid Sierra Madre Oriental matorral community. *J. Arid Environments* 58, 181–202.
- Carlyle-Moses, D. E., Price, A. G., 1999. An evaluation of the Gash interception model in a northern hardwood stand. *J. Hydrol.* 214, 103–110.
- Crockford, R. H., Richardson, D. P., 2000. Partitioning of rainfall into throughfall, stemflow and interception: effect of forest type, ground cover and climate. *Hydrol. Process.* 14, 2903–2920.
- Gash, J. H. C., 1979. An analytical model of rainfall interception in forests. *Q. J. R. Meteorol. Soc.* 105, 43–55.
- Gash, J. H. C., Lloyd, C. R., Lachaud, G., 1995. Estimating sparse forest rainfall interception with an analytical model. *J. Hydrol.* 170, 79–86.
- Gash, J. H. C., Wright, I. R., Lloyd, C. R., 1980. Comparative estimates of interception loss from three coniferous forests in Great Britain. *J. Hydrol.* 48, 89–105.
- Gómez, J. A., Giráldez, J. V., Fereres, E., 2001. Rainfall interception by olive trees in relation to leaf area. *Agricultural Water Management*. 49, 65–76.
- Hamada, S., Ohta, T., Hiyama, T., Kuwada, T., Takahashi, A., Maximov, T. C., 2004. Hydrometeorological behavior of pine and larch forests in eastern Siberia. *Hydro. Processes* 18, 23–39.
- Hashino, M., Yao, H., Yoshida, H., 2002. Studies and evaluations on interception processes during rainfall based on a tank model. *J. Hydrol.* 255, 1–11.
- Herwitz, S. R., Slye, R. E., 1995. Three-dimensional modeling of canopy tree interception of wind-driven rainfall. *J. Hydrol.* 168, 205–226.
- Hutjes, R.W.A., Wierda, A., Veen, A.W.L., 1990. Rainfall interception in the Tai Forest, Ivory Coast: application of two simulation models to a humid tropical system. *J. Hydrol.* 114, 259–275.
- Jetten, V.G., 1996. Interception of tropical rainforest: performance of a canopy water balance model. *Hydrol. Proc.* 10, 671–685.
- Kelliher, F. M., Lloyd, J., Arneth, A., Byers, J.N., McSeveny, T. M., Milukova, I., Grigoriev, S., Panfyorov, M., Sogatchev, A., Varlargin, A., Ziegler, W., Bauer, G., Schulze, E. D., 1998. Evaporation from a central Siberian pine forest. *J. Hydrol.* 279–296.
- Kuraji, K., Tanaka, N., 2003. Rainfall interception studies in tropical forests. *J. Jan For. Soc.* 85, 18–28. (In Japanese with English Summary)
- Lankreijer, H. J. M., Hendriks, M. J., Klaassen, W., 1993. A comparison of models simulating rainfall interception of forests. *Agr. For. Meteorol.* 64, 187–199.
- Link, T. E., Unsworth, M. and Marks, D., 2004. The dynamics of rainfall interception by a seasonal temperate rainforest. *Agric. For. Met.* In press.
- Liu, S. 1997. A new model for the prediction of rainfall interception in forest canopies. *Ecological Modeling* 99, 151–159.
- Llorens, P., Poch, R., Latron, J., Gallart, F., 1997. Rainfall interception by a *Pinus sylvestris* forest patch overgrown in a Mediterranean mountainous abandoned area 1. Monitoring design and results down to the event scale. *J. Hydrol.*, 199, 331–345.
- Llorens, P., Gallart, F., 2000. A simplified method for forest water storage capacity measurement. *J. Hydrol.* 240, 131–144.

- Ohta, T., Hiyama, T., Tanaka, H., Kuwada, T., Maximov, T. C., Ohata, T., Fukushima, Y., 2001. Seasonal variation in the energy and water exchanges above and below a larch forest in eastern Siberia. *Hydrol. Processes* 15, 1459–1476.
- Park, H., Hattori, S., Kang, H., 2000. Seasonal and inter-plot variations of stemflow, throughfall and interception loss in two deciduous broad-leaved forests. *J. Jap. Soc. Hydrol. Water Res.* 13, 17–30.
- Rodrigues, R. R., Martins, S. V., de Barros, L. C., 2004. Tropical rain forest regeneration in an area degraded by mining in Mato Grosso State, Brazil. *For. Ecol. Manage.* 190, 323–333.
- Rutter, A. J., Kershaw, K. A., Robins, P. C., Morton, A. J., 1971. A predictive model of rainfall interception in forests: derivation of the model from observations in a plantation of Corsican pine. *Agr. Meteorol.* 9, 367–384.
- Shiraki, K., 1997. Errors in water flow measurements using a tipping bucket. Proceedings of the 108th Annual Meeting of the Japanese Forestry Society, 305. (In Japanese)
- Shiraki, K., 2004. Compensation of tipping-bucket flow meters. *J. Jap. Soc. Hydrol. Water Res.* 17, 159–162. (In Japanese with English Summary)
- Shuttleworth, W. J., Gash J. H. C., Lloyd, C. R., Moore, C. J., Roberts, J. M., 1984. Eddy correlation measurements of energy partition for Amazonian forest. *Quart. J. R. Met. Soc.* 110, 1143–1162.
- Shuttleworth, W. J., Gash J. H. C., Roberts, J. M., Nobre, C. A., Molion, L. C. B., Ribeiro, M. N. G., 1991. Post-deforestation Amazonian climate: Anglo-Brazilian research to improve prediction. *J. Hydrol.* 129, 71–85.
- Silva, I. C., Okumura, T., 1996. Throughfall, stemflow and interception loss in a mixed white oak forest. (*Quercus serrata* Thunb.) *J. For. Res.* 1, 123–129.
- Takanashi, S., Kosugi, Y., Tanaka, H., Tanaka, K., 2003. Evapotranspiration from a Japanese cypress forest during and after rainfall. *J. Japan Soc. Hydrol. & Water Resour.* 16, 268–283. (In Japanese with English Summary)
- Tsukamoto, Y., Tange, I., Minemura, T., 1988. Interception loss from forest canopies. *Rolling Land Research.* 6, 60–82. (In Japanese with English Summary)
- Valente, F., David, J. S., Gash, J. H. C., 1997. Modelling interception loss for two sparse eucalypt and pine forests in central portugal using reformulated Rutter and Gash analytical models. *J. Hydrol.* 190, 141–162.

Table 1. Summary of the observation sites

Table 2. Summary of rainfall events and meteorological conditions for the analysis period

Fig. 1. PAI (plant area indices) related to the slopes and y-sections of regressions between gross rainfall and throughfall and gross rainfall and stemflow.

Fig. 2. Relationship between mean rainfall intensity and interception rate for each rainfall event.

Fig. 3. Relationship between the interception rate and gross rainfall (a) or the duration of rainfall events (b). The symbols are separated according to rainfall intensity.

Fig. 4. Relationship between wind speed and interception rate. Wind speed is the mean value during and for 10 hours after rainfall events.

Fig. 5. Relationship between PAI and interception rate. The subscripts represent the following studies:

a: Carlyle-Moses and Price (1999), b, d: Carlyle-Moses (2004)

c, h, i: Lankreijer *et al.* (1993), e, f: Valente *et al.* (1997),

g, k: Park *et al.* (2000), j: Silva and Okumura (1996), l: Link *et al.* (2004)

Fig. 6. Relationship between the estimated latent heat sum of flux (LH) used for interception loss and net all-wave radiation (Rn). The net all-wave radiation represents the accumulated values during and for 5 hours after rainfall events.

Fig. 7. Time series of air-temperature differences observed at two levels and hourly hyetographs. Air-temperature differences were calculated by subtracting air temperature at the lower level from that at the upper level.

Fig. 8. Relationship between the saturation deficit and wind speed based on interception rate for rainfall events with a rainfall intensity of less than 1.0 mm hr^{-1} . Symbols are separated according to the interception rate.

Table 1

	Siberia		Japan				
	L1	P4	P1	P2	P3	Qa	Qs
Degrees latitude	62°15' N	62°14' N	39°40' N	39°40' N	39°40' N	35°10' N	35°9' N
Degrees longitude	129°37' E	129°37' E	140°56' E	140°56' E	140°56' E	137°11' E	136°58' E
Vegetation	<i>Larix cajanderi</i>	<i>Pinus sylvestris</i>	<i>Pinus densiflora</i>	<i>Pinus densiflora</i>	<i>Pinus densiflora</i>	<i>Quercus acutissima</i>	<i>Quercus serrata</i>
Observation period	May 10, 2000 - May 10, 2000	May 1, 2000 - May 1, 2000	May 1, 2000 - May 1, 2000	Aug 1, 2002 - Aug 1, 2001	-	Oct 25, 2003	Oct 31, 2001
Average temperature							
during observation	13.2	14.8	19.4	19.4	19.4	-	22.2
period (°C)							
Gross precipitation							
during observation	126.5	126.5	931.4	931.4	931.4	442.0	721.5
period (mm)							
Plot size (m ²)	50 × 50	50 × 50	30 × 30	30 × 30	30 × 30	20 × 20	50 × 50
Stand density							
(stem ha ⁻¹)	840	1492	1444	1678	355	350	2852
Average tree height (m)							
(high tree only)	18	10	11	13	23	14	18
PAI (m ² m ⁻²)	3.71	2.80	4.44	4.25	3.74	3.54	5.18
Number of throughfall							
collectors	10	10	8	8	8	5	12
Number of stemflow							
collectors	6	8	5	12	6	5	14
Number of sample trees							
for sap flow	4	4	-	5	-	-	6
measurement							

Table 2

	Siberia		Japan				
	L1	P4	P1	P2	P3	Qa	Qs
Number of events	13	9	14	8	14	11	16
Ratio of throughfall to rainfall (%)	71.3	64.3	82.3	80.4	82.6	72.4	78.7
Ratio of stemflow to rainfall (%)	0.003	0.028	5.2	2.7	3.3	2.5	3.0
Ratio of interception loss to rainfall (%)	29	36	13	17	14	24	18
Amount of rainfall (mm)	59.13	49.75	152.2	269	174.6	428	735.4
Average rainfall intensity (mm h^{-1})	0.60	0.60	1.1	1.1	1.1	2.3	2.3
Average rainfall per event (mm)	4.5	5.5	10.9	33.6	12.5	26.75	50.5
Total rainfall duration (hr)	102.0	72.0	356.0	226.0	356.0	228	221
Average event time (hr)	7.8	8.0	25.4	28.3	25.4	14.3	20.1
Average saturation deficit (kg kg^{-1})	0.13	0.15		0.15		0.15	
Average temperature ($^{\circ}\text{C}$)	12.7	12.1		21.4		20.9	
Average humidity (%)	87.8	84.1		88.5		89.2	
Average wind speed (m s^{-1})	2.67	2.76		1.39		1.14	
Average net radiation ($\text{W m}^{-2} \text{ hr}^{-1}$)	68.2	62.9		58.2		43.0	

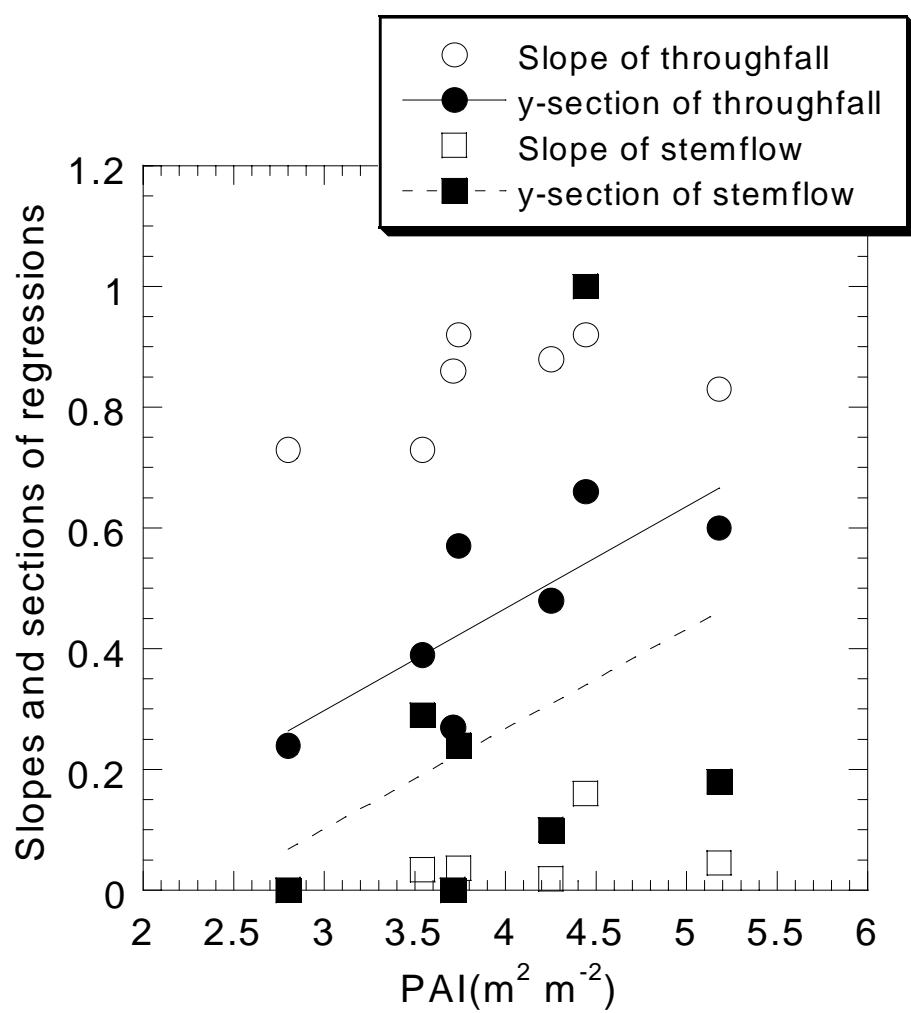


Fig. 1

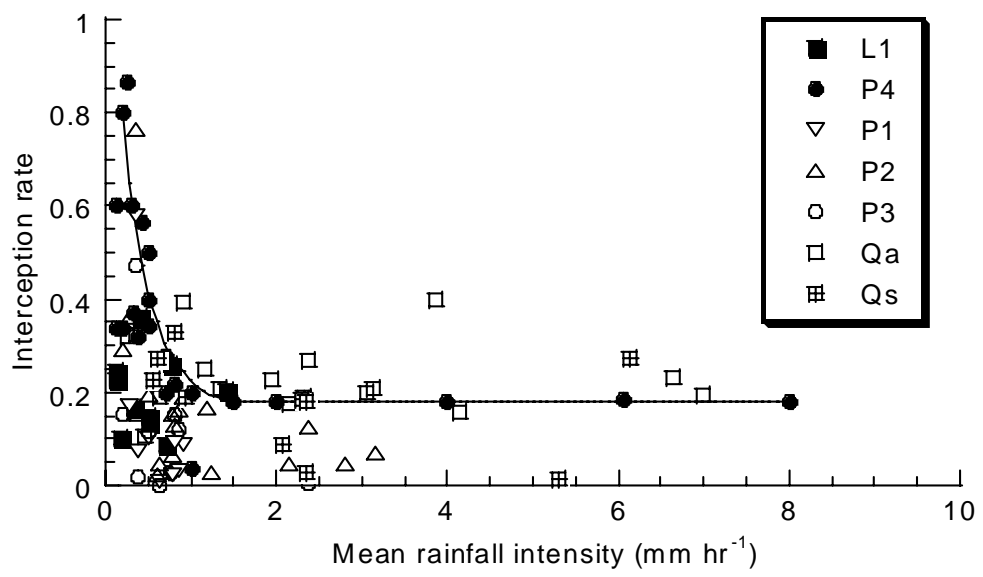
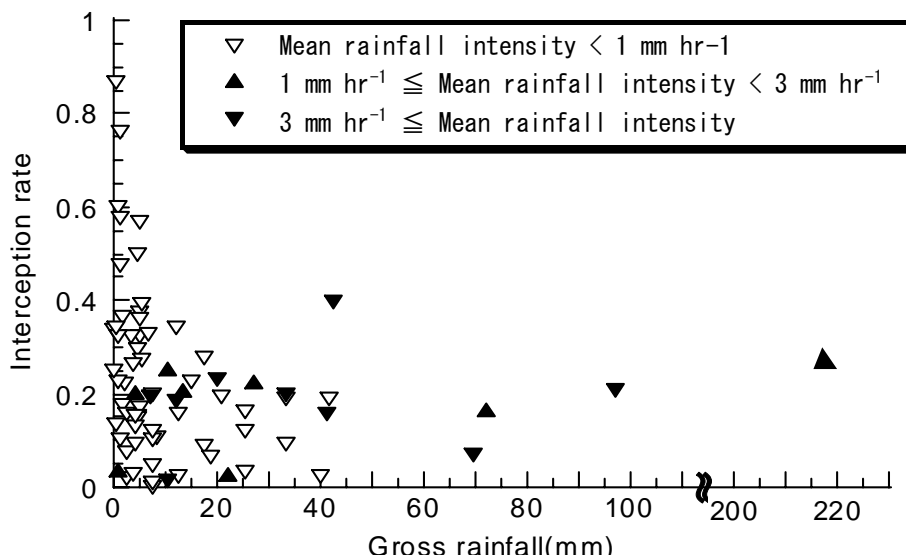
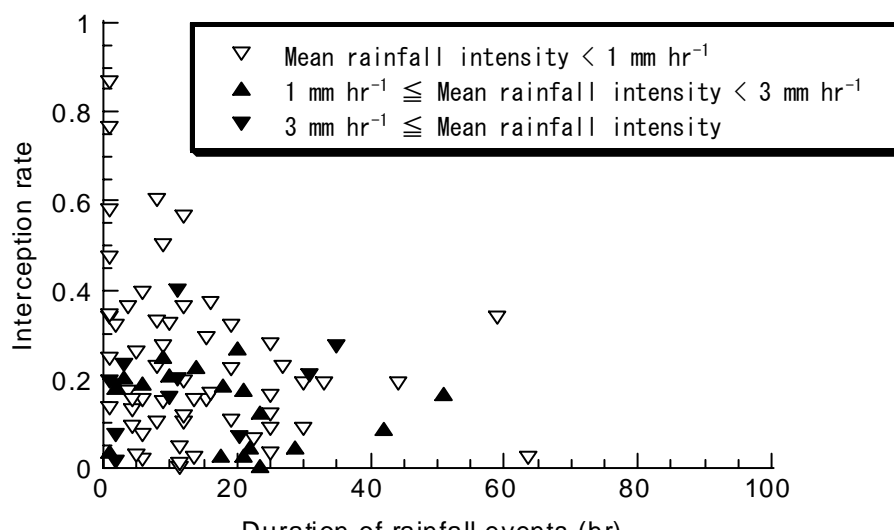


Fig. 2



(a)



(b)

Fig. 3

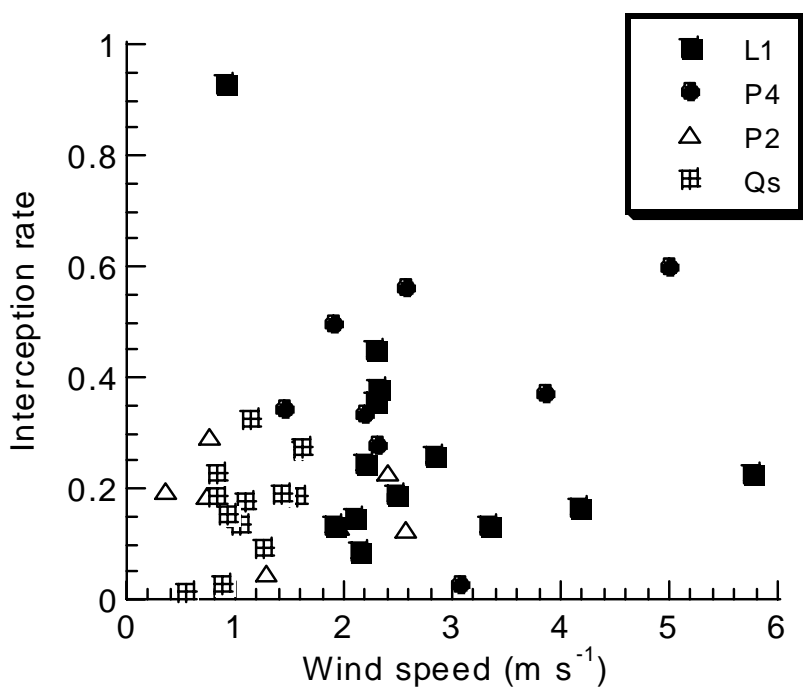


Fig.4

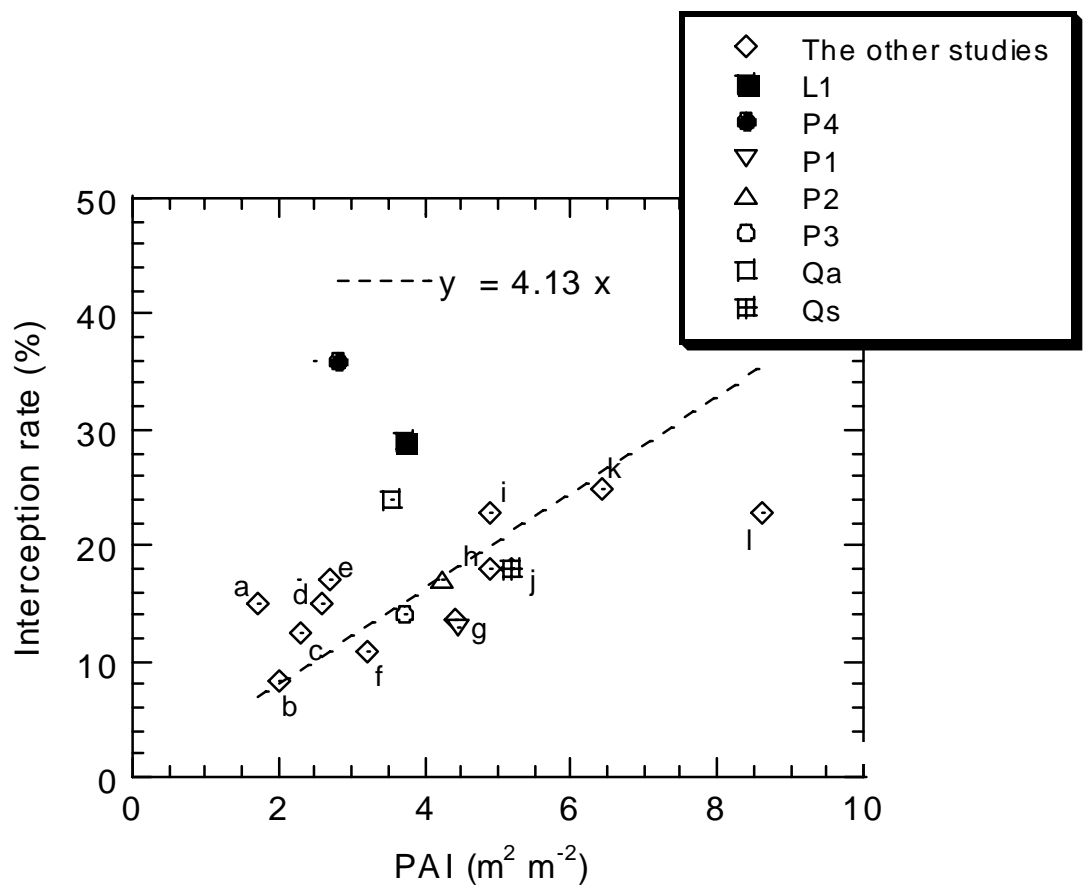


Fig. 5

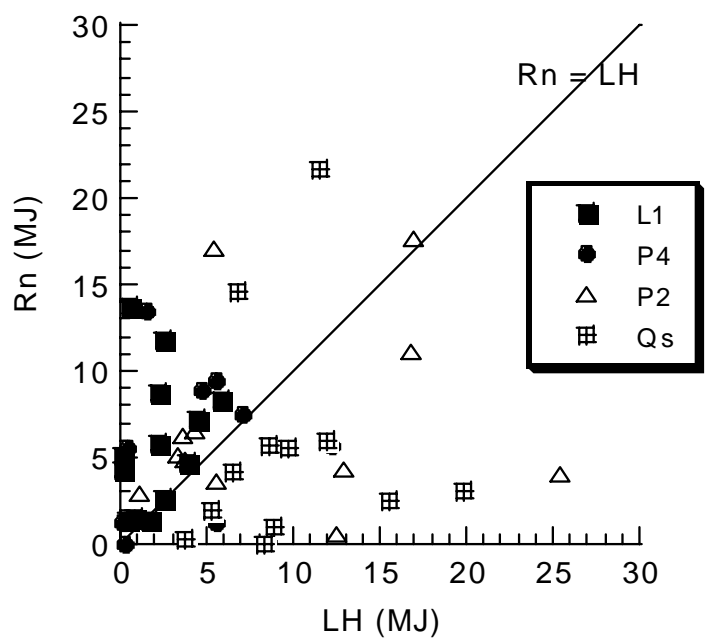


Fig. 6

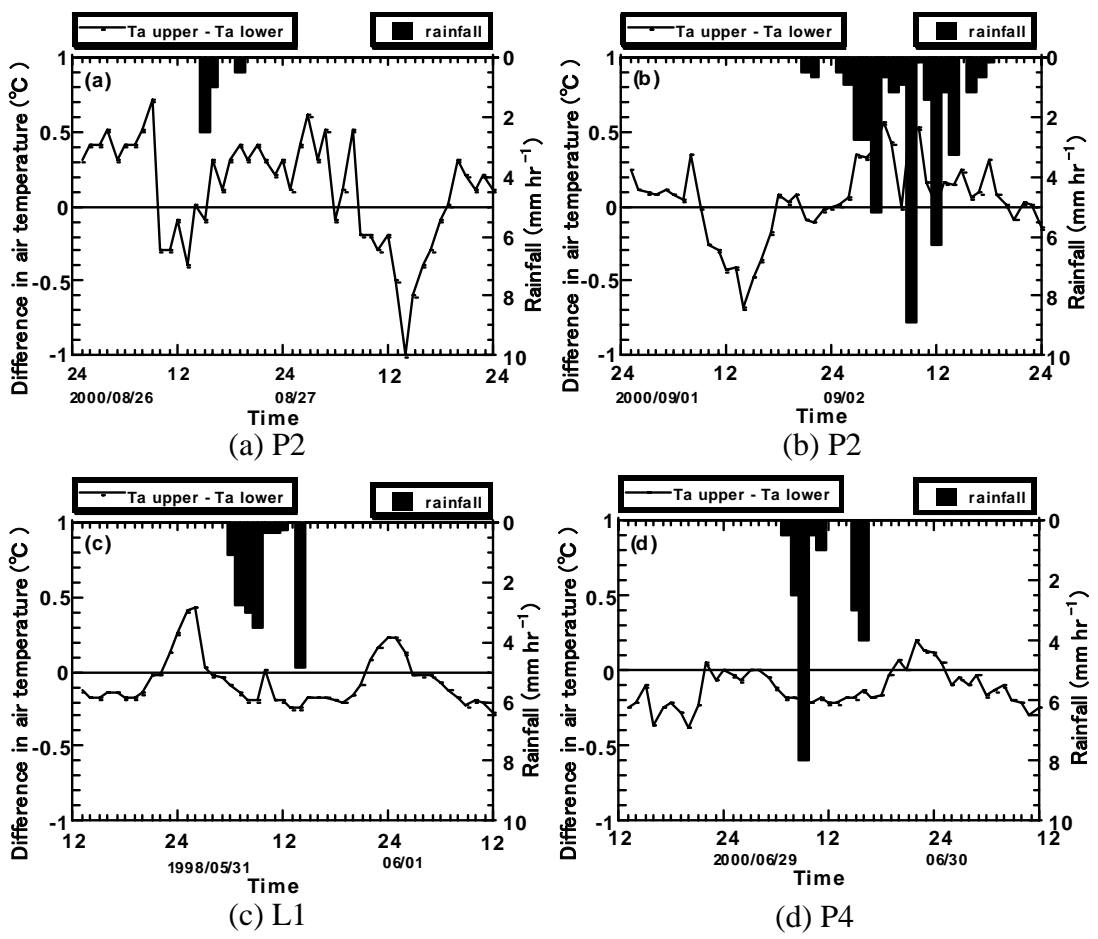


Fig. 7

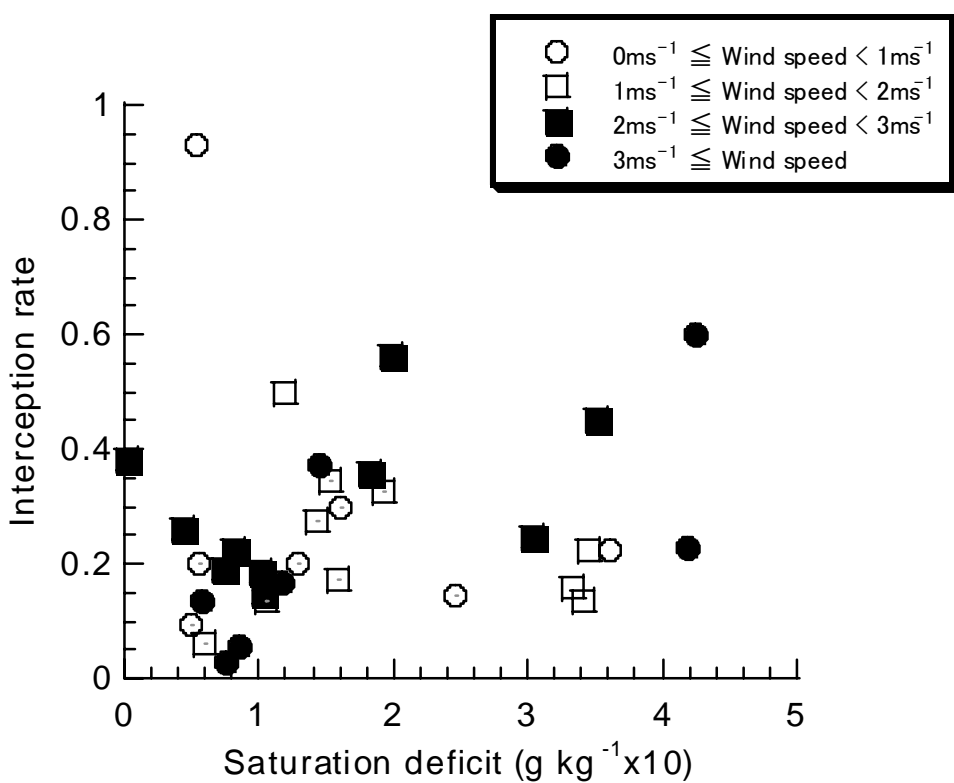


Fig. 8